HHS Public Access

Author manuscript

J Am Coll Cardiol. Author manuscript; available in PMC 2015 July 02.

Published in final edited form as:

J Am Coll Cardiol. 2015 March 10; 65(9): 892–900. doi:10.1016/j.jacc.2014.12.027.

Human Ventricular Unloading Induces Cardiomyocyte Proliferation

Diana C. Canseco, PhD[*], **Wataru Kimura, PhD**[*], **Sonia Garg, MD**[*], **Shibani Mukherjee, PhD**[†], **Souparno Bhattacharya, MS**[‡], **Salim Abdisalaam, PhD**[‡], **Sandeep Das, MD**[*], **Aroumougame Asaithamby, PhD**[‡], **Pradeep P.A. Mammen, MD**[*], and **Hesham A. Sadek, MD, PhD**[*]

[*]Department of Internal Medicine, University of Texas Southwestern Medical Center, Dallas, Texas

[†]Department of Psychiatry, University of Texas Southwestern Medical Center, Dallas, Texas

[‡]Department of Radiation Oncology, University of Texas Southwestern Medical Center, Dallas, Texas

Abstract

Background—The adult mammalian heart is incapable of meaningful regeneration after substantial cardiomyocyte loss, primarily due to the inability of adult cardiomyocytes to divide. Our group recently showed that mitochondria-mediated oxidative DNA damage is an important regulator of postnatal cardiomyocyte cell cycle arrest. However, it is not known whether mechanical load also plays a role in this process. We reasoned that the postnatal physiological increase in mechanical load contributes to the increase in mitochondrial content, with subsequent activation of DNA damage response (DDR) and permanent cell cycle arrest of cardiomyocytes.

Objectives—The purpose of this study was to test the effect of mechanical unloading on mitochondrial mass, DDR, and cardiomyocyte proliferation.

Methods—We examined the effect of human ventricular unloading after implantation of left ventricular assist devices (LVADs) on mitochondrial content, DDR, and cardiomyocyte proliferation in 10 matched left ventricular samples collected at the time of LVAD implantation (pre-LVAD) and at the time of explantation (post-LVAD).

Results—We found that post-LVAD hearts showed up to a 60% decrease in mitochondrial content and up to a 45% decrease in cardiomyocyte size compared with pre-LVAD hearts. Moreover, we quantified cardiomyocyte nuclear foci of phosphorylated ataxia telangiectasia mutated protein, an upstream regulator of the DDR pathway, and we found a significant decrease in the number of nuclear phosphorylated ataxia telangiectasia mutated foci in the post-LVAD hearts. Finally, we examined cardiomyocyte mitosis and cytokinesis and found a statistically significant increase in both phosphorylated histone H3-positive, and Aurora B-positive

Reprint Requests and Correspondence: Dr. Hesham A. Sadek, UT Southwestern, Internal Medicine/Cardiology, 6000 Harry Hines Boulevard, NB10.230A, Dallas, Texas 75039. hesham.sadek@utsouthwestern.edu OR Dr. Pradeep P.A. Mammen, UT Southwestern Medical Center, Division of Cardiology/Department of Internal Medicine, Heart Failure, VAD, & Heart Transplant Program, 5323 Harry Hines Boulevard, Dallas, Texas 75390. pradeep.mammen@utsouthwestern.edu.

Appendix For supplemental figures, please see the online version of this article.

cardiomyocytes in the post-LVAD hearts. Importantly, these results were driven by statistical significance in hearts exposed to longer durations of mechanical unloading.

Conclusions—Prolonged mechanical unloading induces adult human cardiomyocyte proliferation, possibly through prevention of mitochondria-mediated activation of DDR.

Keywords

DNA damage response; heart failure; heart regeneration; mechanical unloading; ventricular assist device

Although modest, but measurable, cardiomyocyte turnover occurs in the adult heart (1,2), it is insufficient for the restoration of contractile function after substantial cardiomyocyte loss. In patients with heart failure, persistent pressure or volume overload results in progression of the underlying cardiomyopathy (3,4). Although this cardiac remodeling can be slowed or sometimes reversed by intense pharmacological therapy, this process is often progressive (5). In advanced heart failure patients, left ventricular assist devices (LVADs) result in improved cardiac output, systemic perfusion, and end-organ function (6,7), which have led to an exponential increase in their implantation over the past decade (8,9). Intriguingly, myocardial recovery allowing for LVAD explantation has been reported in small subsets of patients (10-12) and is thought to result from functional recovery of viable myocardium due to a combination of ventricular unloading and pharmacological therapy (13).

Our group recently showed that activation of the DNA damage response (DDR) is an important mechanism of cell cycle arrest in postnatal mammalian cardiomyocytes (14). We showed that the buildup of mitochondrial mass postnatally results in increased reactive oxygen species (ROS) production, oxidative DNA damage, and activation of DDR. Although the relative hyperoxemia of the postnatal heart plays an important role in up-regulation of oxidative metabolism, increased mechanical load is also known to activate cardiac mitochondrial biogenesis (15). We therefore reasoned that mechanical unloading might reverse the metabolic cascade that results in cell cycle arrest of cardiomyocytes. In this respect, human LVAD hearts provide the unique opportunity to perform histological analysis in the same patient in 2 drastically variable physiological states. We conducted this study to test the effect of mechanical unloading on mitochondrial mass, DDR, and cardiomyocyte proliferation in patients who received LVADs.

Methods

Patient Samples

Human heart tissue samples were obtained from patients with advanced heart failure after informed consent under 2 overlapping institutional review board protocols approved by the UT Southwestern Medical Center Clinical Institutional Review Board Committee (Institutional Review Board #STU 092010-193 and #STU 092010-093). The patients had been referred to the UT Southwestern Medical Center Heart Failure, Ventricular Assist Device & Heart Transplant Program for consideration of either implantation of an LVAD and/or a heart transplantation.

Paired heart tissue samples were obtained from each patient: first at the time of LVAD implantation and again at the time of heart transplantation. Pre-LVAD samples were acquired from the left ventricular apex, whereas the post-LVAD samples were obtained from the lateral wall of the left ventricle. Once the left ventricular tissue was removed from the patient, the tissue was either fixed for 48 h in 10% formalin or snap-frozen in liquid nitrogen. The fixed tissue samples were submitted to the UT Southwestern Medical Center Cardiovascular Histological Laboratory for paraffin embedding and processing for various immunohistological studies.

Mitochondrial DNA Quantification by Real-Time Polymerase Chain Reaction

For mitochondrial DNA (mtDNA) quantification, DNA was extracted and purified from tissue samples with proteinase K digestion and subsequent phenol/chloroform extraction. mtDNA was quantified with real-time polymerase chain reaction with the following primers: mtDNA F: CTAAATAGCCCACACGTTCCC; R: AGAGCTCCCGTGAGTGGTTA (targeting a relatively stable site in mitochondrial DNA minimal arc [16]), and nuclear DNA F: GCTGGGTAGCTCTAAACAATGTATTCA; R: CCATGTACTAACAAATGTCTAAAATGGT (targeting single-copy nuclear DNA within the beta-2M gene [16]), using SYBR Green PCR Master Mix and the 7000 Sequence Detection System (Applied Biosystems, Foster City, California). The relative mtDNA copy number was calculated from the ratio of mtDNA copies to nuclear DNA copies per gram of tissue. The relative fold change was then calculated using the $\Delta\Delta C_T$ method.

Protein Extraction from Heart Tissue and Western Blotting

Whole-cell extracts from human heart samples were prepared as described previously (14). Briefly, samples were homogenized in radioimmunoprecipitation assay buffer using a hand-held homogenizer (Thermo Fisher Scientific, Waltham, Massachusetts) on ice for 30 min. Cell extracts were centrifuged at 14,000 rpm for 30 min at 4°C to remove insoluble material. Radioimmunoprecipitation assay buffer contained phenylmethylsulfonyl fluoride, aprotinin (1 (μg/ml), leupeptin (1 μg/ml), pepstatin A (1 μg/ml), sodium fluoride (150 mM), and sodium metavandate (1 mM). Aliquots containing 200 μg protein were resolved by 8% sodium dodecylsulfate-polyacrylamide gel electrophoresis and then transferred onto nitrocellulose membrane at 30 V at 4°C overnight. Membranes were blocked with 5% milk in Tris-buffered saline-0.1% Tween 20) at room temperature for 20 min and incubated with different antibodies in 5% milk in Tris-buffered saline-0.1% Tween 20 at 4°C overnight. Membranes were subsequently washed 3 times for 5 min each with Tris-buffered saline-0.1% Tween 20, and then incubated with horseradish peroxidase-conjugated secondary antibodies (anti-mouse/rabbit/goat) in 5% milk for 2 h at room temperature. The primary antibodies used for Western blotting were as follows: phosphorylated ataxia telangiectasia mutated (pATM) protein; 10H11.E12) (sc-47732, mouse, 1:500, Santa Cruz Biotechnology, Dallas, Texas) and cardiac troponin T (13-11, mouse, 1:10,000, Thermo Fisher Scientific, Richardson, Texas). Quantification analysis of the Western blot signal was done using ImageJ (National Institutes of Health, Bethesda, Maryland).

Immunostaining

Samples for immunostaining were prepared as described previously (14). Briefly, after antigen retrieval with 1 mM ethylenediamine tetraacetic acid containing 0.05% Tween in boiling water, sections were blocked with 10% serum from the secondary antibody host animal and 0.3% Triton-X100, and incubated with primary antibodies overnight at 4°C. Sections were subsequently washed with phosphate-buffered saline (PBS) and incubated with corresponding secondary antibodies conjugated to Alexa Fluor 488 or 555 (Life Technologies, Carlsbad, California). Primary antibodies used were as follows: anti-phosphorylated histone H3 (pH3); Ser10 (#06-570, 1:100, Millipore, Billerica, Massachusetts); anti-Aurora B (A5102, 1:25, Sigma, St. Louis, Missouri); anti-troponin T, Cardiac Isoform Ab-1, Clone 13-11 (MS-295-P1, 1:100, Thermo Fisher Scientific); anti-sarcomeric alpha-actinin (ab68167, 1:100, Abcam, Cambridge, Massachusetts); and anti-pATM (sc-47739,1:100, Santa Cruz Biotechnology).

Cell Size-Wheat Germ Agglutinin Staining

After antigen retrieval, slides were rinsed 3 times in PBS and then incubated overnight at 4°C with troponin T antibody. The following day, the slides were rinsed 3 times with PBS and incubated for 1 h at room temperature with a primary antibody against wheat germ agglutinin conjugated to 50 μg/ml Alexa Fluor 488 (Life Technologies) and secondary antibody for troponin T. Slides were then rinsed in PBS and mounted in Vectashield (Vector Laboratories, Burlingame, California). To quantify cell size, images at 20× were captured, and ImageJ (National Institutes of Health) was used to determine the area of each cell. Quantitative analyses involved the counting of multiple fields from 3 independent samples per group (∼50 cells per field assessed, total ∼250 cells per group).

Image Acquisition and pATM Foci Quantification

Analysis and quantification of pATM were performed of images captured by a high-resolution LSM 510 Meta laser scanning confocal microscope (Carl Zeiss Inc., Thornwood, New York) equipped with a 63× 1.4 NA Plan-Apochromat oil immersion objective (Carl Zeiss Inc.). Images were taken at z-sections (24 sections) at 0.35-μm intervals using the 488 nm (Alexa 488, Life Technologies), 543 nm (Alexa 555, Life Technologies) and 405 nm (for 2-[4-amidinophenyl]-1H-indole-6-carboxamidine) lasers. The tube current of the 488-nm argon laser was set at 6.1 Å. The laser power was typically set at 3% to 5% transmission with the pinhole opened to 1 to 2 Airy units. The z-sections were subsequently assembled using Imaris software (Bitplane, South Windsor, Connecticut) and then used for further analysis. To count pATM foci, we used the spot detection function of the Imaris software, which determined the spatial position along the x-axis, y-axis, and z-axis and the intensity of the pATM focus that the spot represents. We confirmed the accuracy of foci counting using the same software's colocalization function and observed >99% colocalization of the detected spots with pATM foci. For each sample, the average number of foci per myocyte was quantified for images of 10 to 13 fields.

Image Acquisition for pH3 Quantification

Analysis and quantification of pH3-positive cells were performed using fluorescent microscopy and high-resolution confocal microscopy as described in the preceding section. Only cells displaying a positive pH3 signal in the nucleus, with z-stacking-confirmed 2-(4-amidinophenyl)-1H-indole-6-carboxamidine and actinin colocalization in the same cell were counted. Mitotic cardiomyocytes were counted only if a pH3-positive nucleus was entirely within the boundaries of an actinin-positive cell as determined by continuous actinin staining surrounding the nucleus. False-positive cells with unclear colocalization of pH3 with either 2-(4-amidinophenyl)-1H-indole-6-carboxamidine or actinin or with punctate pH3 staining were excluded.

Statistical Analysis

Pre- and post-LVAD samples were compared using the paired Student *t* test. To assess the impact of dependence on the assumption of normality, a sensitivity analysis was performed using the nonparametric Wilcoxon signed rank test for matched pairs. Results of the nonparametric sensitivity analyses were similar to those of the primary analyses for all comparisons (data not shown). On the basis of previous research suggesting a lack of change in myocardial viability with short (2 to 3 months) LVAD duration (17), an a priori stratification was performed at an LVAD duration of 6 months or less (group 1, short LVAD duration) versus longer than 6 months (group 2, long LVAD duration). Results are expressed as mean ± SEM. Statistical analyses were performed using SAS version 9.2 (SAS Institute, Cary, North Carolina). All statistical tests were 2-tailed with $p < 0.05$ considered statistically significant.

Results

This study included 10 patients (3 female and 7 male) from whom we were able to collect matched tissue samples pre- and post-LVAD at the time of heart transplantation. The average age of these patients was 51 years, and 2 of the patients have since died. The etiology of cardiomyopathy included nonischemic, ischemic, familial, and chemotherapy-induced cardiomyopathies. The duration of left ventricular mechanical unloading with the LVAD ranged from 1 to 25 months (Figure 1A). Quantification was performed on the entire population, as well as on groups 1 and 2.

To test the effect of mechanical unloading with an LVAD on cardiomyocyte mitochondrial content, we analyzed mtDNA in ventricular chambers with or without LVAD support. Quantitative real-time polymerase chain reaction analysis of mtDNA copy number standardized to nuclear DNA copy number in post-LVAD tissue samples showed a decrease of up to 60% compared with matched pre-LVAD samples (n = 10) (Central Illustration A, Figure 1B). Interestingly, heart failure patients maintained on LVADs for longer than 6 months (group 2) (Figure 1B) showed a greater decrease in mtDNA content compared with patients with LVADs for less than 6 months (group 1) (Figure 1B), indicating that mtDNA content progressively decreases with longer LVAD duration.

We then examined the effect of ventricular unloading on cardiomyocyte size. To test this, we performed anti-wheat germ agglutinin staining to visualize cardiomyocyte boundaries and to facilitate measurement of cardiomyocyte cell size (Central Illustration B, Figure 1C, Online Figure S3A). A decrease of as much as 45% in cardiomyocyte cell size in post-LVAD ventricles compared with pre-LVAD ventricles was observed, suggesting that ventricular unloading can reverse cardiomyocyte hypertrophy in the human heart. Consistent with the effect of longer LVAD duration on reduction of mitochondrial mass, a statistically significant decrease in cardiomyocyte size was only observed in patients with LVADs for longer than 6 months (group 2).

As we previously showed (14), reduced mtDNA content is suggestive of lower mitochondrial ROS level and, as a consequence, reduced oxidative DNA damage. Importantly, due to significant variability in timing of access to tissue samples (investigators did not have immediate access to tissue at the time of harvesting), measuring ROS was not feasible in these human samples. We hypothesized that ventricular unloading reduces activation of the DDR, which we previously found to be an important mediator of cardiomyocyte cell cycle arrest (14). To examine the activation of the DDR in cardiomyocytes of pre-LVAD or post-LVAD hearts, we used immunofluorescence and high-resolution confocal microscopy to quantify nuclear pATM (Central Illustration C, Figure 2, Online Figure S3B), which is recruited to DNA lesion foci and acts as an upstream regulator of the DDR pathway (18). Although cardiomyocytes of patients with shorter durations of LVAD (group 1) did not show a statistically significant difference in the number of nuclear pATM foci, cardiomyocytes from patients with longer durations of LVAD (group 2) showed a significant decrease in the number of nuclear pATM foci, indicating that the DDR is deactivated after prolonged ventricular unloading (Figure 2). These findings were also supported by quantitative Western blot analysis, which revealed a trend toward down-regulation of pATM levels in protein extracts from hearts with longer LVAD durations (Online Figures S1A and S3C). However, this analysis did not reach statistical significance, likely due to inclusion of noncardiomyocytes in the protein extract (compared with the more specific quantification of pATM foci in cardiomyocyte nuclei).

When mammalian cardiomyocytes exit the cell cycle postnatally, they display an increase in mitochondrial mass, cell size, and DDR activation (14), all of which are decreased after long-term unloading, as described earlier. Therefore, we next tested whether pressure unloading reverses cardiomyocyte cell cycle arrest. We examined cardiomyocyte mitosis by immunostaining using anti-pH3 Ser 10, a specific marker of G2-M progression. Quantification of the number of cardiomyocytes with nuclear pH3 signal (Central Illustration D, Figure 3A, upper panels) revealed a statistically significant increase in pH3-positive cardiomyocytes in all post-LVAD patients combined. This increase was not significant in shorter duration LVAD patients (group 1), consistent with the lack of an appreciable decrease in pATM foci in these cardiomyocytes. However, the number of pH3-positive cardiomyocytes was significantly increased in patients with longer LVAD duration (group 2) (Figure 3A, Online Figure S3D). It is important to note that myocyte proliferation was confirmed by stringent criteria, using high-resolution confocal z-stacking microscopy, the gold standard method for identification of cardiomyocyte nuclei (Figure 3A, upper panels). These findings were further supported by quantification of the localization of the

cytokinesis marker Aurora B kinase to the cleavage furrow between 2 cardiomyocytes (19) (representative images of all samples examined in this study are shown in Online Figure S2). Quantification of confocal images indicated a significant increase of Aurora B-positive cells in all post-LVAD samples combined, with a similar statistically significant increase with longer LVAD duration (Central Illustration D, Figure 3B, Online Figures 2 and 3E). It is important to note here that we also used strict z-stack quantification without the use of 2-dimensional imaging. This was necessary because Aurora B can be found in the cleavage furrow between 2 myocytes that are not necessarily in the same horizontal plane (as demonstrated in the figure inset). This technique markedly increased the sensitivity and specificity of identifying true cardiomyocyte cytokinesis. Collectively, these results indicate that ventricular unloading, especially for longer durations, induces cell cycle re-entry in adult human cardiomyocytes.

Discussion

Cell cycle re-entry of mammalian adult cardiomyocytes has been previously demonstrated in animal models (20-25); however, similar findings have not been reported in humans because of the difficulty of performing such studies. The current study builds on our recent work (14), which suggested that cardiomyocyte cell cycle exit is a regulated process and likely to play a protective role against replication in the setting of oxidative DNA damage. We previously demonstrated that, by enhancing mitochondrial ROS production and oxidative DNA damage, the postnatal hyperoxic environment is an important mediator of cardiomyocyte cell cycle exit. We now show that mechanical loading is an important regulator of mitochondrial biogenesis, DDR, and cardiomyocyte cell cycle in the adult human heart. Importantly, although the effects of mechanical unloading on cardiomyocyte size and nucleation were previously described (10,12,26), the current study indicates that the reverse remodeling that occurs with unloading may represent a switch from hypertrophic to hyperplastic growth. The current study highlights the association between the duration of LVAD mechanical support and molecular changes in cardiomyocytes, where decreased DDR and induction of cardiomyocyte proliferation were restricted to longer LVAD durations. Consistent with these observations, a recent study showed no post-LVAD change in myocardial viability after a short duration on LVAD, highlighting the need for a better understanding of the temporal effects of mechanical unloading on cardiomyocyte cell cycle and heart regeneration (17).

The current findings are consistent with those of previous reports suggesting that functional recovery on an LVAD may be possible (4,27,28), although variations in protocol, duration on LVAD, and outcomes highlight the need for in-depth examination of myocardial viability and contractile function after mechanical unloading.

Study Limitations

Despite the significance of these findings, the current study falls short of providing a clear understanding of the mechanism of cell cycle entry after mechanical unloading. Other limitations also include the small sample size, in particular in group 1, and the difference in anatomic location of pre-LVAD and post-LVAD samples (apex and lateral wall,

respectively). More importantly, although there is clear evidence of cardiomyocyte proliferation in the unloaded human heart, it is unclear whether this leads to an appreciable regenerative effect and restores contractile function in the failing heart. Certainly, any attempts at reloading post-LVAD ventricles must take into account the significant cardiomyocyte atrophy that occurs after prolonged mechanical unloading, which will likely hamper any appreciable restoration of cardiac output without reactivation of cardiomyocyte hypertrophy.

Conclusions

Prolonged mechanical unloading of the human heart results in a switch from hypertrophic to hyperplastic cardiomyocyte growth.

Supplementary Material

Refer to Web version on PubMed Central for supplementary material.

Acknowledgments

The authors thank Dr. Milton Packer for his insightful remarks as well as Dr. James Richardson and John Shelton for their valuable input.

This work was supported by NIH R01-HL102478 to Dr. Mammen and by R01-HL115275 to Dr. Sadek. Dr. Sadek also received support from the Foundation for Heart Failure Research, New York. All other authors have reported that they have no relationships relevant to the contents of this paper to disclose.

References

1. Bergmann O, Bhardwaj RD, Bernard S, et al. Evidence for cardiomyocyte renewal in humans. Science. 2009; 324:98–102. [PubMed: 19342590]
2. Kajstura J, Urbanek K, Perl S, et al. Cardiomyogenesis in the adult human heart. Circ Res. 2010; 107:305–15. [PubMed: 20522802]
3. Zafeiridis A, Jeevanandam V, Houser SR, et al. Regression of cellular hypertrophy after left ventricular assist device support. Circulation. 1998; 98:656–62. [PubMed: 9715858]
4. Drakos SG, Kfoury AG, Hammond EH, et al. Impact of mechanical unloading on microvasculature and associated central remodeling features of the failing human heart. J Am Coll Cardiol. 2010; 56:382–91. [PubMed: 20650360]
5. Gheorghiade M, Pang PS. Acute heart failure syndromes. J Am Coll Cardiol. 2009; 53:557–73. [PubMed: 19215829]
6. Gupte AA, Hamilton DJ, Cordero-Reyes AM, et al. Mechanical unloading promotes myocardial energy recovery in human heart failure. Circ Cardiovasc Genet. 2014; 7:266–76. [PubMed: 24825877]
7. Birks EJ. Molecular changes after left ventricular assist device support for heart failure. Circ Res. 2013; 113:777–91. [PubMed: 23989719]
8. Miller LW, Pagani FD, Russell SD, et al. HeartMate II Clinical Investigators. Use of a continuous-flow device in patients awaiting heart transplantation. N Engl J Med. 2007; 357:885–96. [PubMed: 17761592]
9. Kirklin JK, Naftel DC, Pagani FD, et al. Sixth INTERMACS annual report: a 10,000-patient database. J Heart Lung Transplant. 2014; 33:555–64. [PubMed: 24856259]
10. Ambardekar AV, Buttrick PM. Reverse remodeling with left ventricular assist devices: a review of clinical, cellular, and molecular effects. Circ Heart Fail. 2011; 4:224–33. [PubMed: 21406678]

11. Kirklin JK, Naftel DC, Kormos RL, et al. Fifth INTERMACS annual report: risk factor analysis from more than 6,000 mechanical circulatory support patients. J Heart Lung Transplant. 2013; 32:141–56. [PubMed: 23352390]
12. Nsair A, Liem DA, Cadeiras M, et al. Molecular basis of recovering on mechanical circulatory support. Heart Fail Clin. 2014; 10(1 Suppl):S57–62. [PubMed: 24262353]
13. Birks EJ, George RS, Hedger M, et al. Reversal of severe heart failure with a continuous-flow left ventricular assist device and pharmacological therapy: a prospective study. Circulation. 2011; 123:381–90. [PubMed: 21242487]
14. Puente BN, Kimura W, Muralidhar SA, et al. The oxygen-rich postnatal environment induces cardiomyocyte cell-cycle arrest through DNA damage response. Cell. 2014; 157:565–79. [PubMed: 24766806]
15. Piquereau J, Caffin F, Novotova M, et al. Mitochondrial dynamics in the adult cardiomyocytes: which roles for a highly specialized cell? Front Physiol. 2013; 4:102. [PubMed: 23675354]
16. Phillips NR, Sprouse ML, Roby RK. Simultaneous quantification of mitochondrial DNA copy number and deletion ratio: a multiplex real-time PCR assay. Sci Rep. 2014; 4:3887. [PubMed: 24463429]
17. Gupta DK, Skali H, Rivero J, et al. Assessment of myocardial viability and left ventricular function in patients supported by a left ventricular assist device. J Heart Lung Transplant. 2014; 33:372–81. [PubMed: 24582837]
18. Jackson SP, Bartek J. The DNA-damage response in human biology and disease. Nature. 2009; 461:1071–8. [PubMed: 19847258]
19. Goto H, Yasui Y, Kawajiri A, et al. Aurora-B regulates the cleavage furrow-specific vimentin phosphorylation in the cytokinetic process. J Biol Chem. 2003; 278:8526–30. [PubMed: 12458200]
20. Bersell K, Arab S, Haring B, et al. Neuregulin1/ ErbB4 signaling induces cardiomyocyte proliferation and repair of heart injury. Cell. 2009; 138:257–70. [PubMed: 19632177]
21. Chen J, Huang ZP, Seok HY, et al. mir-17-92 cluster is required for and sufficient to induce cardiomyocyte proliferation in postnatal and adult hearts. Circ Res. 2013; 112:1557–66. [PubMed: 23575307]
22. Eulalio A, Mano M, Dal Ferro M, et al. Functional screening identifies miRNAs inducing cardiac regeneration. Nature. 2012; 492:376–81. [PubMed: 23222520]
23. Mahmoud AI, Kocabas F, Muralidhar SA, et al. Meis1 regulates postnatal cardiomyocyte cell cycle arrest. Nature. 2013; 497:249–53. [PubMed: 23594737]
24. Sdek P, Zhao P, Wang Y, et al. Rb and p130 control cell cycle gene silencing to maintain the postmitotic phenotype in cardiac myocytes. J Cell Biol. 2011; 194:407–23. [PubMed: 21825075]
25. Xin M, Kim Y, Sutherland LB, et al. Hippo pathway effector Yap promotes cardiac regeneration. Proc Natl Acad Sci U S A. 2013; 110:13839–44. [PubMed: 23918388]
26. Wohlschlaeger J, Levkau B, Brockhoff G, et al. Hemodynamic support by left ventricular assist devices reduces cardiomyocyte DNA content in the failing human heart. Circulation. 2010; 121:989–96. [PubMed: 20159834]
27. Klotz S, Jan Danser AH, Burkhoff D. Impact of left ventricular assist device (LVAD) support on the cardiac reverse remodeling process. Prog Biophys Mol Biol. 2008; 97:479–96. [PubMed: 18394685]
28. Yacoub MH. A novel strategy to maximize the efficacy of left ventricular assist devices as a bridge to recovery. Eur Heart J. 2001; 22:534–40. [PubMed: 11259141]

Abbreviations and Acronyms

DDR	DNA damage response
LVAD	left ventricular assist device
mtDNA	mitochondrial DNA

pATM	phosphorylated ataxia telangiectasia mutated protein
PBS	phosphate-buffered saline
pH3	phosphorylated histone H3
ROS	reactive oxygen species

Perspectives

Competency in Medical Knowledge

Mechanical unloading of the human heart decreases the size of cardiomyocytes and mitochondrial content and, when prolonged, induces cardiomyocyte proliferation through DNA damage response-dependent effects on the cell cycle.

Translational Outlook

Additional studies are needed to explore the regenerative effects on the myocardium of prolonged mechanical unloading.

A Clinical Characteristics

Patient Study#	Age (years)	Sex	Race	Current Vital Status	Etiology of CM	History of CABG?	Duration on LVAD (months)
12	60	F	W	Alive	Chemotherapy	N	2
13	40	F	W	Dead	Nonischemic	N	13
16	38	M	W	Alive	Neuromuscular	N	1
18	60	F	W	Alive	Familial	N	7
20	60	M	W	Dead	Ischemic	Y	14
23	48	M	W	Alive	Nonischemic	N	25
37	71	M	W	Alive	Ischemic	?	7
47	65	M	W	Alive	Nonischemic	N	6
85	30	M	AA	Alive	Nonischemic	N	14
109	66	M	W	Alive	Ischemic	N	7

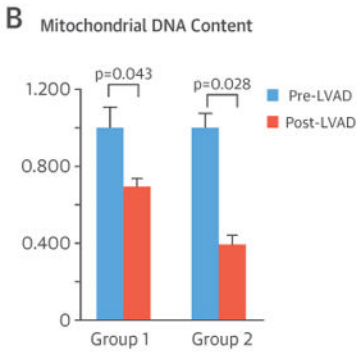

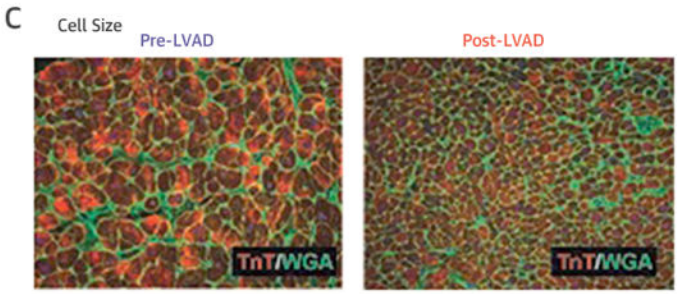

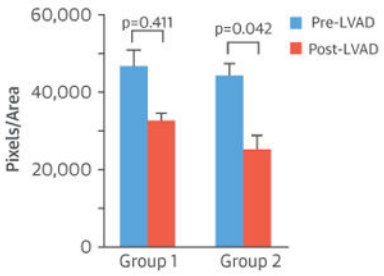

Figure 1. LVAD Support for Heart Failure Patients Leads to Decreased Mitochondrial DNA Copy Number and Cardiomyocyte Cell Size

(A) Samples from various heart failure patients with different durations of LVAD support were used for the study. **(B)** Quantitative polymerase chain reaction analysis showed that in both groups 1 (short LVAD duration; 6 months or less) and 2 (long LVAD duration; longer than 6 months), the mitochondrial DNA copy number was significantly decreased compared with the nuclear DNA copy number in post-LVAD supported hearts versus pre-LVAD supported hearts. **(C)** Cardiomyocyte cell size analyzed by immunostaining using anti-WGA and anti-cardiac TnT antibodies showed a marked decrease in cardiomyocyte size in the overall population as well as in groups 1 and 2. AA = African American; CABG = coronary artery bypass grafting; CM = cardiomyopathy; LVAD = left ventricular assist device; TnT = troponin T; W = white; WGA = wheat germ agglutinin.

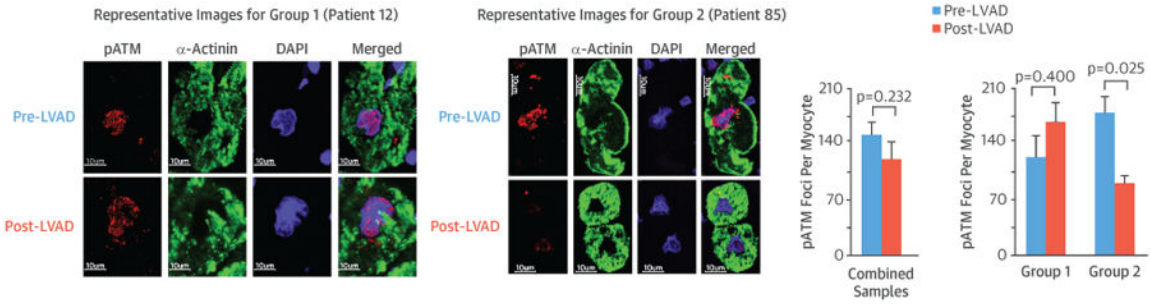

Figure 2. LVAD-Mediated Pressure Unloading Leads to Reduced DDR in Adult Human Cardiomyocytes

High-resolution confocal microscopy of immunostaining with pATM antibody shows a significant decrease in nuclear pATM foci and the DDR only in longer duration group 2 post-LVAD cardiomyocytes. DAPI = 2-(4-amidinophenyl)-1H-indole-6-carboxamidine; DDR = DNA damage response; LVAD = left ventricular assist device; pATM = phosphorylated ataxia telangiectasia mutated protein.

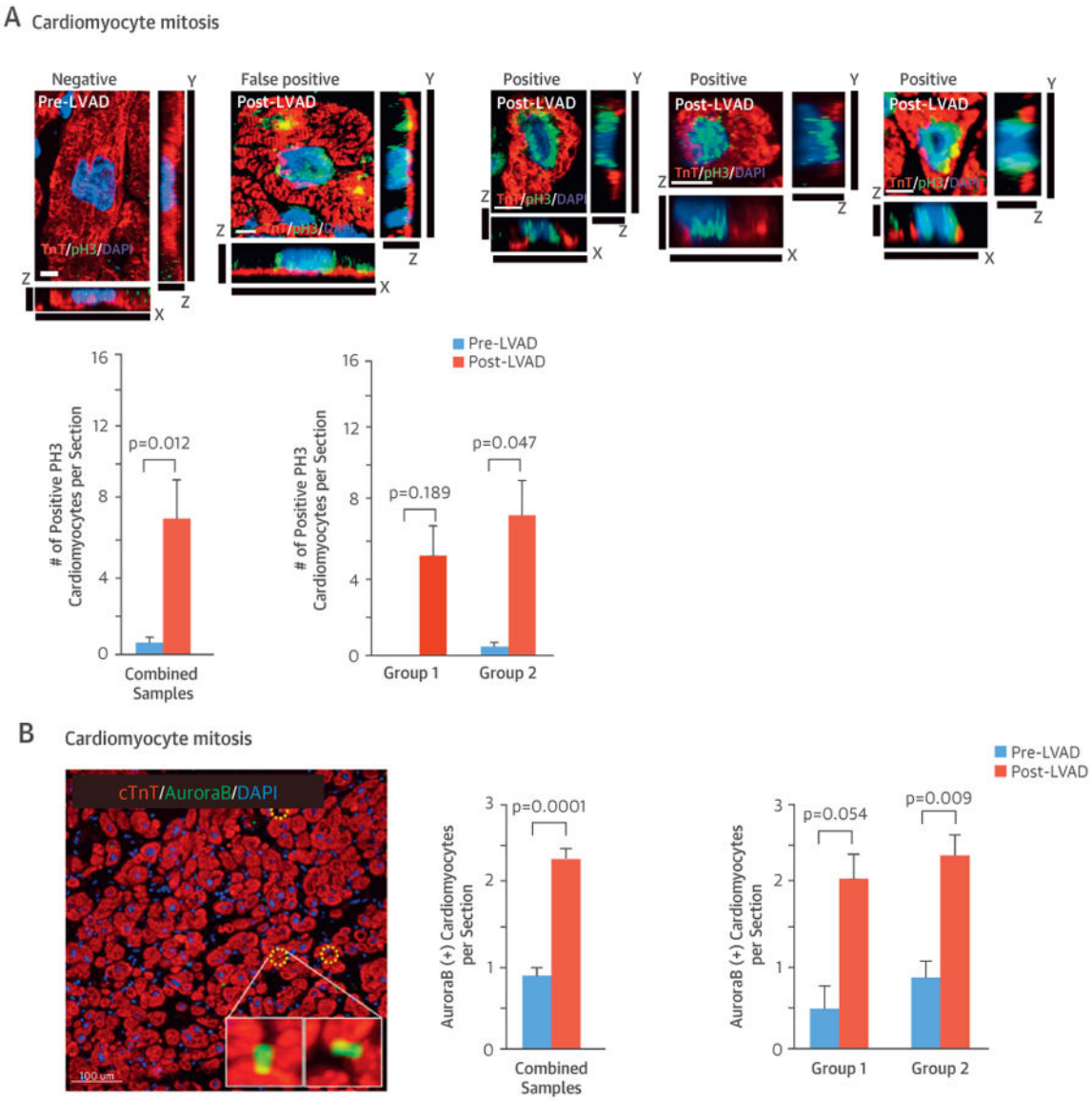

Figure 3. LVAD-Mediated Pressure Unloading Induces Cardiomyocyte Proliferation in Adult Human Heart

(A) Confocal z-stack imaging after pH3 antibody staining showed a significant increase in cardiomyocyte mitosis in the longer duration group 2 LVAD hearts. Scale bar=5 µm. Note that stringent criteria were used for localization of pH3 staining to cardiomyocytes. True- and false-positive examples are provided. **(B)** Confocal z-stack imaging of Aurora B kinase showed a marked increase in cardiomyocyte cytokinesis in the longer duration group 2 LVAD hearts. Scale bar = 100 µm. Note the localization of Aurora B kinase to the cleavage following between 2 cardiomyocytes **(right inset)**. cTnT = cardiac troponin T, PH3 = phosphorylated histone H3; other abbreviations as in Figure 2.

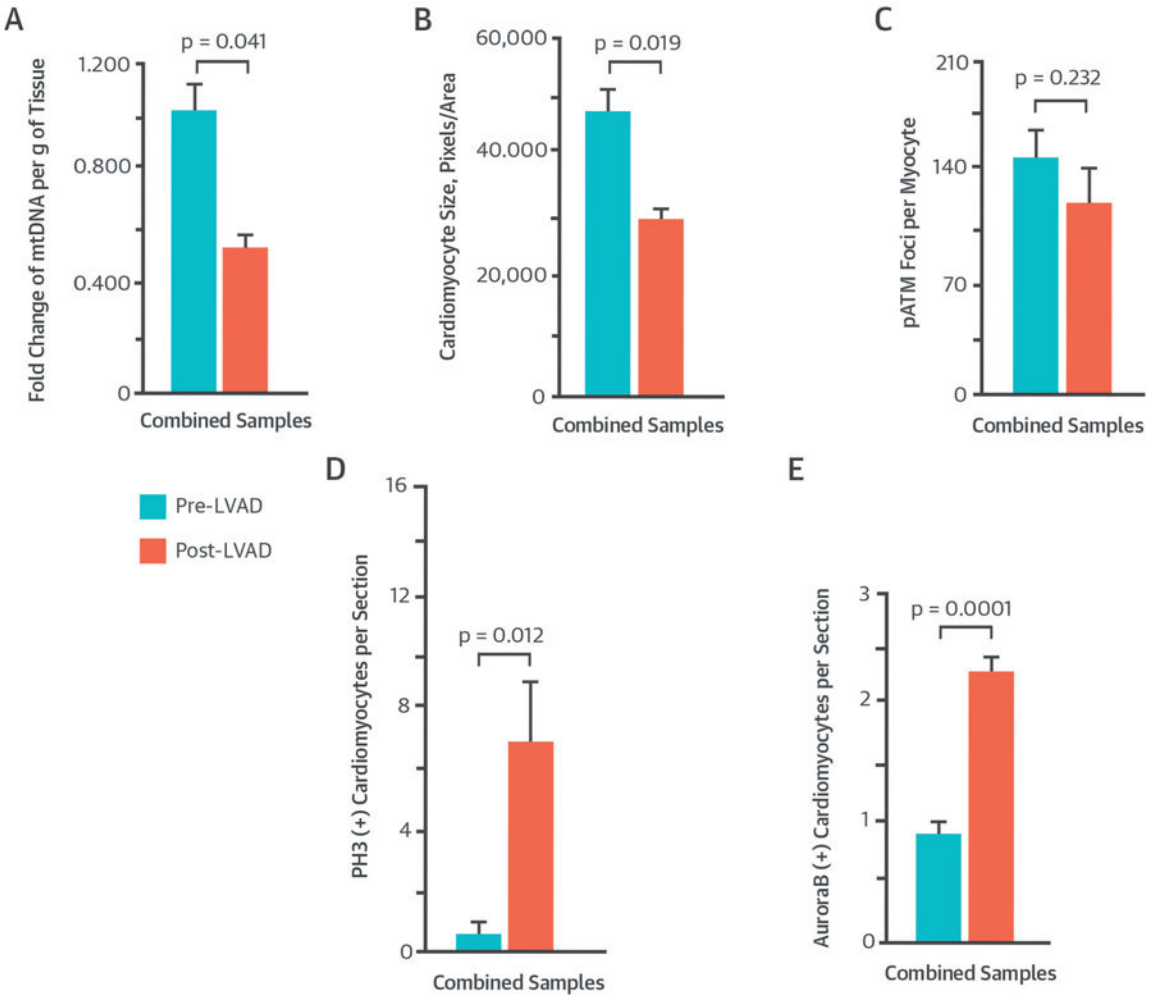

Central Illustration. Cardiomyocyte Proliferation in LVAD Patients: Prolonged Mechanical Unloading Results in a Switch From Hypertrophic to Hyperplastic Cardiomyocyte Growth

Both mtDNA content **(A)** and cell size **(B)** markedly decreased post-LVAD in the combined samples. The DNA damage response was not significantly decreased in the combined samples post-LVAD, as shown by measurements of pixels/area **(C)** and by the number of pATM protein foci per myocyte in the combined samples. Post-LVAD, cardiomyocyte mitosis, shown by increased pH3-positive cardiomyocytes **(D)**, and cardiomyocyte cytokinesis, shown by increased Aurora B localization to cytokinetic furrows **(E)**, were both significantly increased in the combined samples. Collectively, these results suggest that mechanical unloading results in cardiomyocyte cell cycle re-entry. LVAD = left ventricular assist device; mtDNA = mitochondrial DNA; pATM = phosphorylated ataxia telangiectasia mutated protein; PH3 = phosphorylated histone H3.